THE AMERICAN SOCIETY OF MECHANICAL ENGINEERS
345 E. 47th St., New York, N.Y. 10017

97-GT-535

WAKE RECOVERY PERFORMANCE BENEFIT IN A HIGH-SPEED AXIAL COMPRESSOR

Dale E. Van Zante
Iowa State University
Ames, Iowa

John J. Adamczyk
Anthony J. Strazisar
NASA Lewis Research Center
Cleveland, Ohio

Theodore H. Okiishi
Iowa State University
Ames, Iowa

ABSTRACT

This paper addresses the significant differences in compressor rotor wake mixing loss which exist in a stage environment relative to a rotor in isolation. The wake decay for a rotor in isolation is due solely to viscous dissipation which is an irreversible process and thus leads to a loss in both total pressure and efficiency. Rotor wake decay in the stage environment is due to both viscous mixing and the inviscid strain imposed on the wake fluid particles by the stator velocity field. This straining process, referred to by Smith (1993) as recovery, is reversible and for a 2D rotor wake leads to an inviscid reduction of the velocity deficit of the wake. It will be shown that for the rotor/stator spacing typical of core compressors, wake stretching is the dominant wake decay process within the stator with viscous mixing playing a secondary role.

A model for the rotor wake decay process is developed and used to quantify the viscous dissipation effects relative to those of inviscid wake stretching. The model is verified using laser anemometer measurements acquired in the wake of a transonic rotor operated in isolation and in a stage configuration at near peak efficiency and near stall operating conditions. Additional insight is provided by a time-accurate 3D Navier Stokes simulation of the compressor stator flow field at the corresponding stage loading levels. Results from the wake decay model exhibit good agreement with the experimental data. Data from the model, laser anemometer measurements, and simulations indicate that wake straining (stretching) is the primary decay process in the stator passage. The implications of these results on compressor stage design are discussed.

NOMENCLATURE

A_t	time average operator
A_y	pitchwise average operator
b, b_o	1/2 wake width, initial 1/2 wake width
D, D_o	relative wake depth, initial relative wake depth
h	stator pitch
K	flux of kinetic energy of the first order unsteady velocity field
$L_{in,exit}$	wake length
R	recovery parameter
$(\bar{s} - c)$	distance, see Figure 2
T	rotor blade passing period
U	free stream velocity
$U_{inlet,exit}$	nozzle inlet and exit velocities
U_o, V_o	time average velocity, initial free stream velocity
u,v	axial and tangential velocity components
x_1, x_2	stator inlet and exit plane
β_{abs}	absolute flow angle
β_{exit}	absolute flow angle at stator exit
β_{rel}	flow angle relative to rotor
$\beta_\infty, \beta_{-\infty}$	upstream, downstream absolute flow angle
Δ	perturbation parameter
$\left(\frac{\varepsilon}{U\theta}\right)$	eddy viscosity
θ, θ_o	momentum thickness, initial momentum thickness
χ_1, χ_2	total pressure mixing loss at inlet,exit of stator

INTRODUCTION

Rotor wakes are an important source of unsteadiness and loss in axial compressors. The decay (mixing) rate of a rotor wake in isolation determines the rate of accrual of mixing loss, a decrement of the useful work done by the rotor. The accurate prediction of rotor wake decay for an isolated rotor is complicated by pressure gradients in the wake (Kool and Hirsch, 1982) and by wake asymmetry (Raj and Lakshminarayana, 1973) due to the turning

Presented at the International Gas Turbine & Aeroengine Congress & Exhibition
Orlando, Florida — June 2–June 5, 1997

and work addition of the rotor. Additionally, free stream pressure gradients also have a large effect on the rate of wake decay (Hill et al., 1963, Nakayama, 1987). The noted studies considered the influences of viscosity, pressure gradients and curvature on decay of a wake or wakes in isolation. However, this paper will show that in the stator passage of a compressor stage other wake decay mechanisms dominate.

The unsteady process of wake/blade row interaction has commonly been described using kinematic models of wake chopping and transport such as those discussed by Smith (1966), Kerrebrock and Mikolajczak (1970), and Tweedt, et al.(1985). Additional mechanisms that act on the blade wakes in the stage environment are now receiving attention. Originally Smith (1966) proposed one important mechanism, which he called wake recovery, that occurs in a downstream blade row and can be beneficial to performance. Wake recovery is the attenuation (or amplification) of the wake velocity profile by processes other than viscous dissipation occurring inside of a blade row. For a two-dimensional wake passing through a compressor stator row, wake recovery leads to rotor wake decay through a reversible process. In this way the loss due to viscous wake decay is not suffered.

Smith (1966) was the first to propose a simple model for the wake recovery mechanism. He later expanded on his ideas of wake stretching and developed a quantitative model of performance enhancement (Smith, 1993) due to wake recovery. Smith also provided circumstantial evidence that wake recovery benefits exist using data from a low-speed four stage research compressor that exhibited higher pressure rise and efficiency with closer axial blade spacing (Smith, 1970).

In a different approach, Adamczyk (1996) showed that the wake recovery process is related to wake vorticity field kinematics and can be estimated from linear theory. He showed that for the 2D, incompressible, inviscid case, the amount of rotor wake decay or recovery in loss of total pressure in the stator row was directly related to the difference of disturbance (wake) kinetic energy flux entering and leaving a blade row and that having a wake pass through a blade row prior to mixing the wake does reduce mixing loss. With the assumption of thin airfoils at zero incidence, the model of Adamczyk reduces to the model of Smith which is based on wake lengths.

Deregel and Tan (1996) used a first of a kind 2D time-accurate Navier Stokes simulation to study rotor wake recovery for a range of stator blade design parameters and found that mixing loss was reduced due to the inviscid stretching of the wakes in the stator passage. Pressure rise was also increased because of the reduction of disturbance kinetic energy from the inlet to outlet of the passage.

Some early axial compressor stage measurements (Ding, 1982), although limited in the number of axial and circumferential inter-blade measurement points, provided a first step in the experimental observation of wake/blade row interactions in high-speed axial flow machines. Ding noted large flow acceleration and deflection within a short axial distance thus hinting at the strong wake/blade row interactions which occur in a close-coupled high-speed compressor stage. More extensive measurements of rotor wakes convecting through a stator row have been acquired in a low-speed axial compressor (Stauter, 1991), a high-speed axial stage (Dunker, 1983), a high-speed multi-stage compressor (Williams, 1988), and a transonic fan stage (Hathaway, 1986). However, none of these data have been analyzed from the viewpoint of wake recovery.

This paper provides evidence of rotor wake recovery in a high-speed axial compressor stage using experimental data supplemented by numerical simulations. Interrogation of the experimental data and the results of a 3D time-accurate simulation of the stator flow field identify wake stretching as the primary wake decay mechanism within the stator. The wake decay model of Hill et al. (1963) is extended to model the passage of a rotor wake through a stator and forms the basis of a model that includes the effects of wake straining and viscous dissipation on wake decay. Wake decay estimates from this simple model agree well with the measured wake decay. This new wake decay model provides a simple method for predicting the wake decay due to both viscosity and wake stretching by using only stator inlet and exit flow angles and an approximate rotor wake profile. The wake decay trends predicted by the model are used to suggest compressor design practices which can utilize the wake recovery process to reduce stage loss.

WAKE DECAY MODEL

A method for quantifying the wake unsteadiness comes from the analysis of Adamczyk which is used to quantify rotor wake decay (Adamczyk, 1996) without viscous dissipation effects. He showed for 2D, incompressible flow that wake recovery, R, and decrease in wake mixing loss in the absence of viscosity across a stator, $\chi_1 - \chi_2$, can be related to the difference between the flux of kinetic energy of the first order unsteady velocity component entering the stator passage and leaving the stator passage. This can be written:

$$\chi_1 - \chi_2 = K_1 R \qquad \text{(EQ 1)}$$
$$= K_1\left(1 - \frac{K_2}{K_1}\right) + O(\Delta^3)$$

where:

$$K_1 = \frac{1}{2} U_o A_y A_t (u_1^2 + v_1^2)\Big|_{x_1} \qquad \text{(EQ 2)}$$
$$K_2 = \frac{1}{2} U_o A_y A_t (u_1^2 + v_1^2)\Big|_{x_2}$$

and x_1 refers to the stator leading edge plane and x_2 refers to the stator exit plane. A_y is a pitchwise average operator and A_t is a time average operator. The definitions of u_1 and v_1 are illustrated in Figure 1. The disturbance kinetic energy (DKE) is a measure of the deterministic unsteadiness of the flow field at a fixed point in space and is given by $DKE = 0.5 U_o A_t (u_1^2 + v_1^2)$. K is the flux of DKE, $K = A_y(DKE)$. DKE is presented as a percentage of $0.5 U_{tip}^3$ in all figures.

A wake passing through a stator passage is tilted and

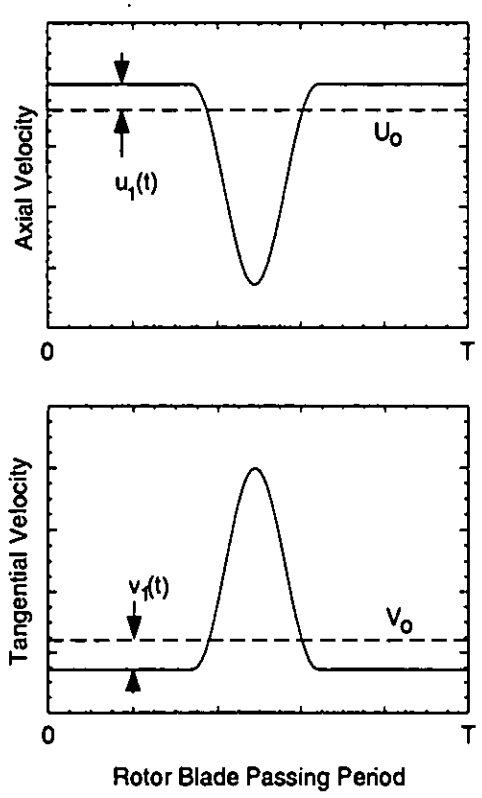

FIGURE 1. Disturbance kinetic energy velocity components.

stretched due to stator circulation (loading) as shown in Figure 2. Smith (1966) proposed the following simple model which is based on wake lengths for the recovery of total pressure mixing loss:

$$R = 1 - \left(\frac{L_{in}}{L_{exit}}\right)^2 \qquad \text{(EQ 3)}$$

In the present work the ratio of wake lengths can be determined from experimental data. In most cases such detailed data is not available and one needs a method to estimate the wake stretching. Smith (1966) proposed a simple method for estimating the wake stretching based on inlet and exit velocity triangles. Adamczyk rediscovered Smith's result as the limit obtained from unsteady thin airfoil theory. The model as formulated by Adamczyk (1996) is:

$$\frac{L_{exit}}{L_{in}} = \left.\frac{\sin(\beta_{rel}-\beta_{abs})}{\cos\beta_{abs}}\right|_{inlet} \left[1 + \frac{2(\bar{s}-c)}{h}\sin(\beta_{exit}) + \left(\frac{(\bar{s}-c)}{h}\right)^2\right]^{\frac{1}{2}} \qquad \text{(EQ 4)}$$

where:

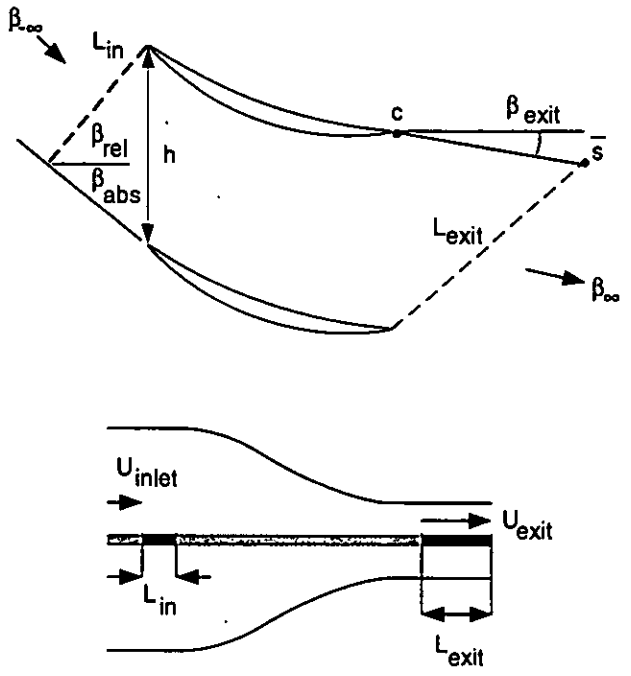

FIGURE 2. Definition of angles and lengths used in the wake stretching model and an illustration of wake stretching in a 2D converging channel.

$$\frac{\bar{s}-c}{h} = \frac{\cos\beta_{rel}}{\sin(\beta_{rel}-\beta_\infty)}\left(\frac{\cos\beta_\infty}{\cos\beta_\infty}\right) - \frac{4(\tan\beta_\infty - \tan\beta_\infty)}{(\cos\beta_\infty + \cos\beta_\infty)^2}\cos\beta_\infty(\cos\beta_\infty)^2 \qquad \text{(EQ 5)}$$

See Figure 2 for definitions of the terms. Angles are positive in the counter-clockwise direction.

Equations 3-5 provide a method for estimating the kinematic contribution of wake stretching to the total rotor wake decay using only inlet and exit velocity triangles and blade geometry information.

Inside the stator passage, wake stretching and viscous dissipation act concurrently on the rotor wake. A method for estimating the viscous contribution to wake decay is obtained from the work of Hill et al. (1963) on turbulent wake decay in steady pressure gradients.

Hill et al. developed a decay model for 2D incompressible turbulent wakes based on a constant eddy viscosity assumption. The model compared well with adverse pressure gradient wake decay measurements and was stated as being equally applicable to favorable pressure gradients. The model is extended to favorable pressure gradients as follows.

The wake stretching which occurs in a stator passage is analogous to the lengthening of a wake segment of constant mass as it passes through an acceleration (converging channel), as shown in Figure 2. For 2D incompressible flow the wake length ratio across the channel is given by:

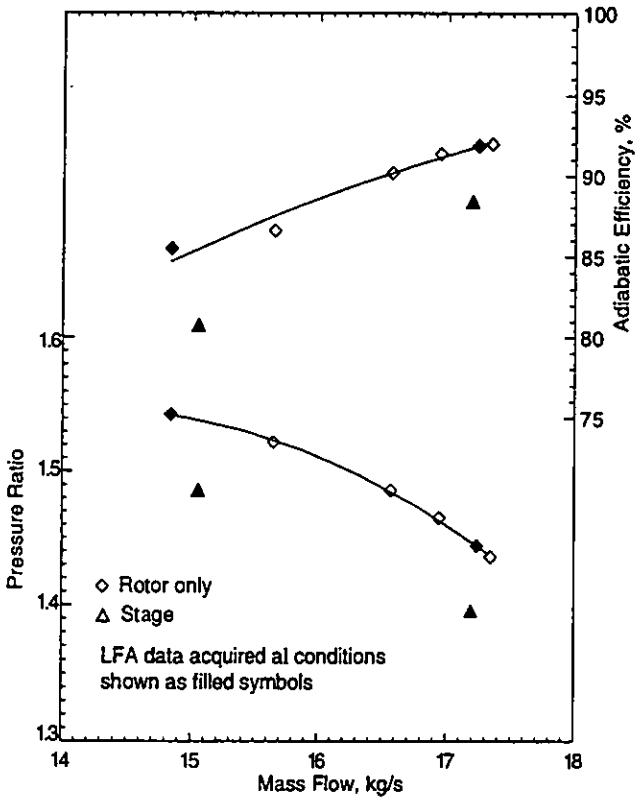

FIGURE 3. Operating map for rotor in isolation and in the stage environment.

$$\frac{L_{exit}}{L_{in}} = \frac{U_{exit}}{U_{inlet}} \qquad \text{(EQ 6)}$$

By choosing the correct velocity ratio for a 2D channel, the lengthening of a wake segment as it convects through that channel can be made to simulate rotor wake lengthening in a stator passage. This is done later in this paper.

The wake decay model taken from Hill et al.'s work can be summarized as:

$$D = \frac{U - U_{min}}{U} \qquad \text{(EQ 7)}$$

where D is the relative wake depth, U is the average of the wake edge velocities (Nakayama, 1987), and U_{min} is the wake center velocity. The wake depth, width, and velocity profile are given by:

$$\frac{D}{D_o} = \left(\frac{U_o}{U}\right)^2\left[1 + \frac{8\pi^2}{\pi^2 - 4}\left(\frac{\varepsilon}{U\theta}\right)\int_{x_o}\frac{U_o}{U}d\left(\frac{D_o^2\, x}{\theta_o}\right)\right]^{-\frac{1}{2}} \qquad \text{(EQ 8)}$$

$$\frac{b}{b_o} = \left(\frac{U_o}{U}\right)^3 \frac{\left(\frac{1}{D_o} - \frac{3}{4}\right)}{\left(\frac{1}{D_o} - \frac{3}{4}\frac{D}{D_o}\right)\frac{D}{D_o}} \qquad \text{(EQ 9)}$$

$$\frac{U - u}{U} = D\frac{1}{2}\left[1 + \cos\left(\pi\frac{y}{b}\right)\right] \qquad \text{(EQ 10)}$$

Eqn. 8 estimates the change in relative wake depth as a function of axial distance and velocity ratio which represents the free stream pressure gradient. Knowing the relative wake depth, the wake width can be computed from Eqn. 9. The wake velocity profile is computed from Eqn. 10. The eddy viscosity used in the model is constant with axial distance and equal to 0.044 (Hill et al., 1963).

Equations 3 through 10 represent the complete wake decay model which incorporates the effects of both wake stretching and viscous dissipation. The predicted wake decay from the model will be compared to measurements of rotor wake decay which were acquired downstream of a high-speed axial-compressor rotor in isolation and in the stage environment.

TEST COMPRESSOR

The measurements were acquired in the NASA Lewis single-stage axial-flow compressor facility. The test stage consisted of NASA Rotor 35 and NASA Stator 37. The rotor had 36 blades, a hub-tip radius ratio of 0.70, an aspect ratio of 1.19, a tip solidity of 1.3, and an axial chord of 3.56 cm at the hub. The rotor tip clearance gap was 1.5% of axial chord. The stator had 46 blades, a tip solidity of 1.3, an aspect ratio of 1.26, and an axial chord of 3.57 cm at the hub. The gap/chord ratio for the stage varies from 18% at the hub to 31% at the tip based on rotor hub chord. The design and blade coordinates are found in Reid and Moore (Oct. 1978). The original test stage consisted of Rotor 37 and Stator 37 with Stator 37 configured for optical access. At the beginning of the test program Rotor 37 was damaged from the implosion of an optical access window. Rotor 35, which used the same flowpath geometry, was substituted for Rotor 37. Because of the lower pressure ratio of Rotor 35, data were acquired at 80% of design speed to avoid choking problems in the stator. An Average Passage code analysis (Adamczyk, 1985) was used to match the stator to the rotor at the lower operating speed. Based on this analysis, the stator stagger angle was decreased by four degrees.

Data were taken with Rotor 35 in isolation at a tip speed of 363 m/s (80% design speed) at two operating conditions, near peak efficiency (PE) and near stall (NS). The stage data were acquired at conditions for which the rotor exit tip static pressures in the rotor only and stage configuration were matched. The rotor only and stage PE and NS operating points are shown in Figure 3. The shaded symbols represent operating points at which LFA data were acquired.

INSTRUMENTATION AND MEASUREMENT TECHNIQUES

Compressor massflow was measured using a calibrated orifice plate located far upstream of the compressor. Performance measurements were acquired using conventional static pressure and total pressure/temperature probes located upstream and downstream of the compressor. In the stage configuration, the downstream probes were traversed circumferentially across one stator

pitch. At each span, the circumferential profiles of total temperature were mass averaged to obtain a radial profile. Similarly, the circumferential profiles of total pressure were energy averaged by converting them to their enthalpy equivalents and then mass averaging across the stator pitch. Overall performance was calculated by mass and energy averaging total temperature and total pressure, respectively, across the annulus (Reid and Moore, Nov. 1978). Measurement uncertainties are: massflow ±0.3 kg/s; flow angle ±0.5 degrees, total pressure ±0.01 N/cm^2, total temperature ±0.6 K.

A large window, which conformed to the 3D shroud contour, provided optical access to the flowfield from one rotor chord upstream of the rotor to one stator chord downstream of the stator. Laser fringe anemometer (LFA) measurements were made at 75% span from the hub across one stator pitch; see Figure 4. Detailed pitchwise surveys were acquired from the rotor trailing edge (TE) through 20% stator chord, at 50% stator chord, and at 90%, 110%, 120% stator chord. Typically there were 15 to 18 measurement locations in a pitchwise survey at each axial position. The 110% stator chord plane is the closest axial position to the STE where a complete pitchwise data survey was acquired and thus was used as the stator exit condition in calculations. Three streamwise surveys were done at 4.2%, 50%, and 87.5% of stator pitch (not % gap). The axial locations at which rotor only data were acquired are also shown. The error in the LFA measurements is approximately ±1.0 m/s for absolute velocity and ±0.5 degrees in absolute flow angle.

The LFA was configured as a two-channel laser system which acquired axial and tangential velocities simultaneously. For each velocity measurement the rotor position was determined from a shaft angle encoder and the data placed into the window corresponding to that shaft angle position. There were 184 windows across one rotor blade pitch. Typically 40,000 to 60,000 individual velocity measurements were acquired for each survey point. Since the measurements were not evenly distributed over all of the windows, the total number of measurements was chosen so as to insure that there were a minimum of 100 measurements in any window. The LFA data are ensemble averaged using one rotor blade pitch as the time scale. See Strazisar et al. (1989) for more detail on the LFA data acquisition and reduction technique.

NUMERICAL SIMULATIONS

3D time-averaged Navier Stokes simulations of the compressor stage operating at the PE and NS conditions were first generated using the Average Passage code developed by Adamczyk (1985). 3D, time-accurate, Reynolds-averaged Navier-Stokes simulations of the stator flow field were then generated using a code by Chen et al. (1994). The unsteady code uses a time-shifted non-uniform upstream boundary condition that simulates the relative movement of the incoming wake. The code uses a Baldwin-Lomax turbulence model. The upstream boundary condition was obtained from the rotor flow field portion of the Average Passage simulation. The initial solution for the stator flow field was obtained from the stator portion of the Average Passage simulation. In all CFD simulations the stator count was increased from 46 to 48 to achieve a 3:4 rotor stator blade count in preparation for

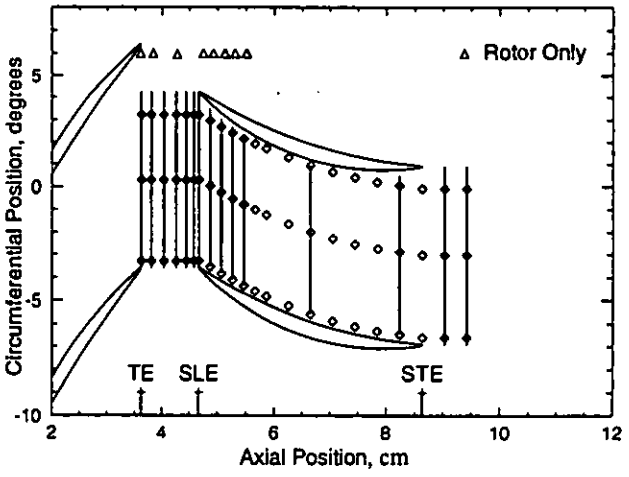

FIGURE 4. LFA measurement locations for rotor and stage environment with axial locations of rotor trailing edge (TE), stator leading edge (SLE), and stator trailing edge (STE).

running a full stage unsteady simulation using the Chen/Adamczyk code. The grid size used was 101 axial x 51 radial x 43 tangential nodes. The solutions each required approximately 10 hours of Cray C90 cpu time using 224 time steps per rotor blade passing period.

The massflow for the Average Passage simulations was matched to the experiment. The overall simulation performance results are in Table 1.

Table 1: Overall performance results from the numerical simulations.

	Average Passage		Chen/ Adamczyk	
	PE	NS	PE	NS
m (kg/s)	17.2	15.2	17.3	15.0
PR	1.43	1.50	NA	NA
efficiency	85.2	80.1	NA	NA

DATA ANALYSIS

Figure 5 shows examples of the LFA measurements from: a) the time average velocity field and b) the flow field for a particular rotor/stator position for both PE and NS. Figure 6 shows the simulation results from the same viewpoints. The purpose of the simulations was not code validation, but rather to provide a comprehensive data base to aid in the wake decay model and experimental data analysis. The time-average absolute velocities from the LFA data and simulations agreed to within 5%. The time average absolute velocity field shows that the stator is aft loaded at the PE condition and front loaded at the NS condition. The wake kinematics predicted from the simulations agreed well with the experiment as shown in Table 2. Also the unsteady behavior of the

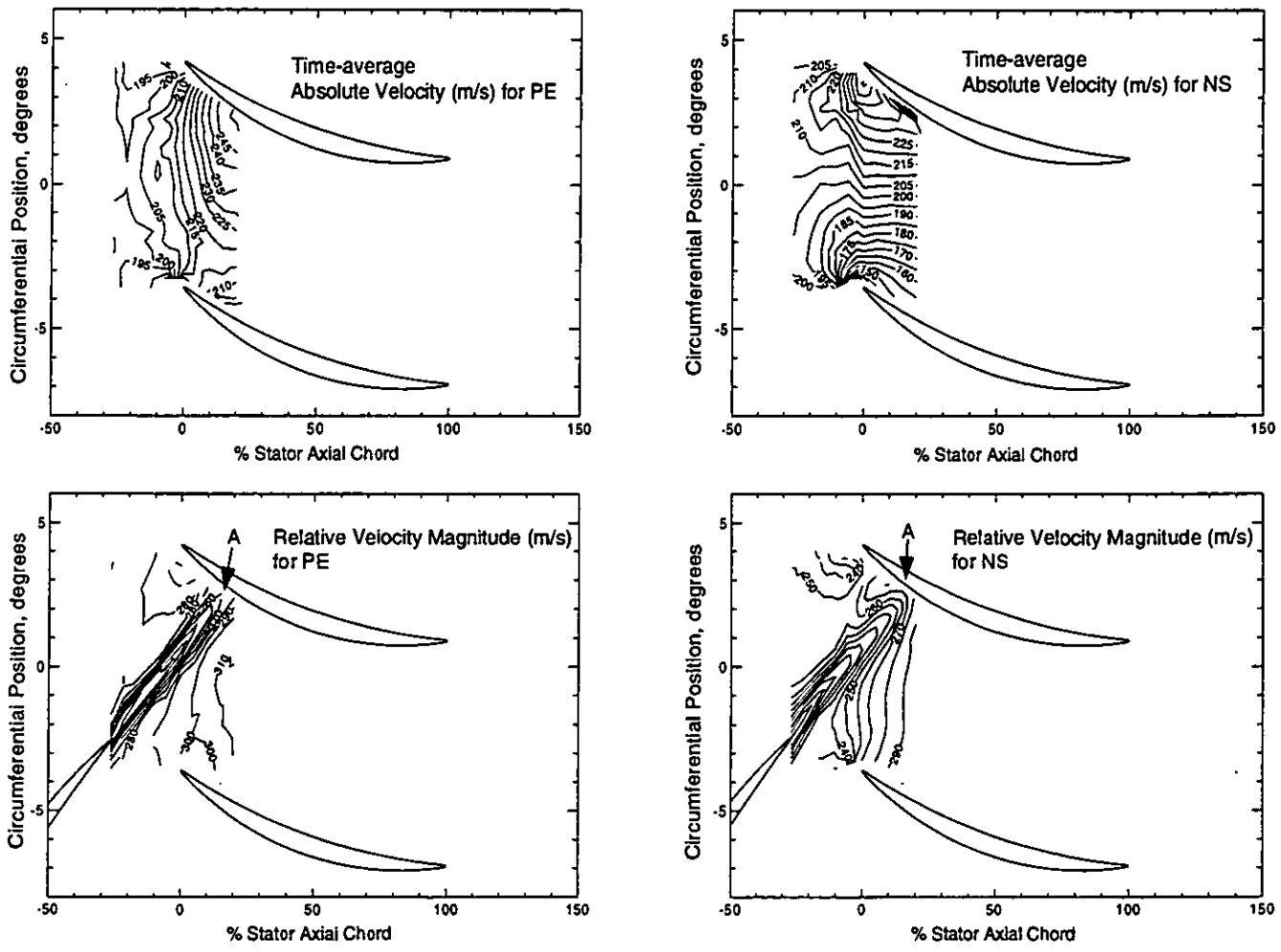

FIGURE 5. Time average absolute velocity (m/s) and relative velocity magnitude (m/s) for a fixed rotor/stator position based on laser anemometer data.

wakes in the simulations was qualitatively the same as for the LFA measurements. Figure 7 shows that the decay of K within the stator is similar for the experiments and simulations. The simulations were therefore considered representative of the experimental observations and valid for use in interpreting the test data.

The kinematic model of wake stretching and the wake decay model are based on 2D incompressible flow assumptions and do not include the effects of either wake drift or radial transport. The validity of using the 2D incompressible assumptions is discussed in the APPENDIX. For the results presented in this paper, wake drift and radial transport are not significant contributors to wake decay.

For practical reasons it is not normally possible to determine wake lengths from experiments or simulations and thus, Eqn. 4 provides a simple and adequate method for determining the wake lengths. Wake length ratios calculated with Eqn. 4 are compared to length ratios obtained directly from experimental and simulation results in Table 2. Compared to the data, the formula underpredicted the wake stretching. The agreement could be improved if a more complete representation of the inviscid wake transport process was used. However, the resulting additional complexity was deemed unnecessary for quantifying the effects of the velocity triangles and cascade geometry on the recovery process.

From the inviscid models of Smith and Adamczyk, the recovery of the rotor wake is proportional to the wake inlet and exit length ratio, $R = 1 - (L_{in}/L_{exit})^2$. A recovery of 1.0 (100%) means that the rotor wake has been completely mixed out in the stator passage by wake stretching and the rotor wake mixing loss possible at the SLE has been completely recovered in a reversible way. The recovery calculated from experimentally measured wake length ratios was 0.64 for PE and 0.78 for NS data. Therefore, the flux of DKE at the stator exit has been reduced and the rotor wake mixing loss possible is reduced by 64% and 78% respectively. For comparison, the recovery due to wake stretching using wake length ratios as calculated from Eqn. 4 is underpredicted by 10% for PE and 14% for NS.

The total reduction in the flux of DKE from SLE to STE, as calculated from experimental data, was 0.71 for PE and 0.82 for NS data; see Figure 7. The further decrease in the flux of DKE above that due to stretching, 7% for PE and 4% for NS, was due to

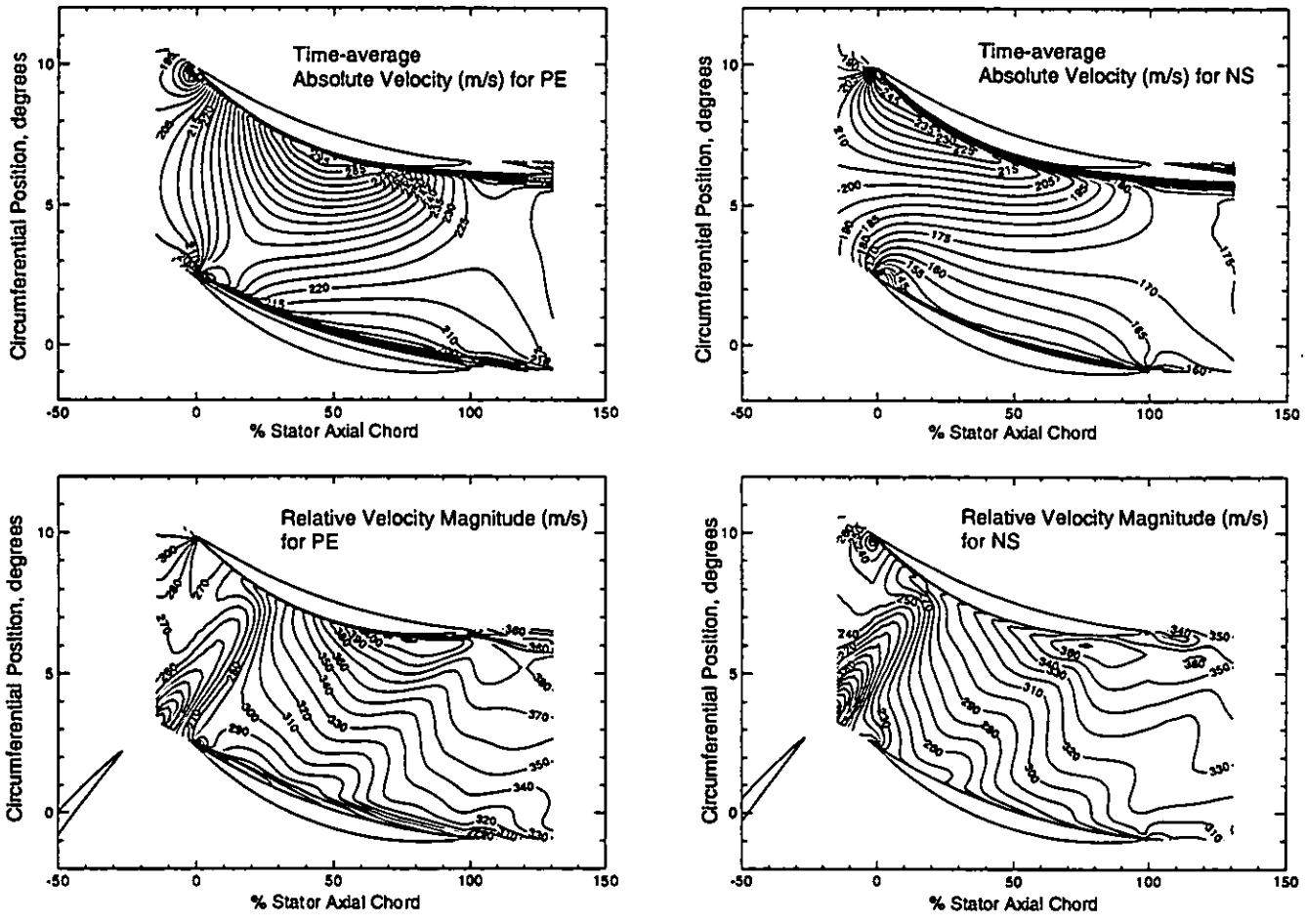

FIGURE 6. Time average absolute velocity (m/s) and relative velocity magnitude (m/s) for a fixed rotor/stator position based on numerical simulations.

viscous dissipation in the stator row. This comparison of the inviscid model recovery predicted from wake lengths to the total measured decrease in DKE strongly indicates that the primary decay mechanism in the stator passage is wake stretching and that viscous dissipation appears to be of secondary importance. In the subsequent discussion it will be shown that the wake decay model (Eqns. 7-10) is consistent with the experimental findings.

The rotor wake profile at the stator leading edge plane at midpitch is used to determine the initial relative wake depth and width needed in the decay model. The wake profiles are shown in Figure 8. Note that the rotor relative velocity magnitude, as shown in the figure, was used for the calculations. The stator midpitch location was chosen to minimize the wake gust/stator response interaction which is not included in the model.

The flow turning through the stator row as determined from the absolute flow angle data, indicated that a linear pressure gradient is a reasonable approximation to the rotor wake stretching that occurs in the stator passage. Eqns. 4 and 5 relate the flow turning to wake stretching. A linear accelerating pressure gradient with x distance, which is represented by U_o/U in Eqn. 8, was thus used in the model such that the velocity ratio at the stator exit was equal to the wake length ratio (see Eqn. 6) as determined from the experimental data.

Table 2: Wake length ratios as measured from the LFA data and numerical simulations and calculated using Eqn. 4.

	Experiment		Simulation	
	measured	Eqn. 4	predicted	Eqn. 4
PE	1.67	1.52	1.62	1.53
NS	2.14	1.74	2.05	1.81

To determine a relative wake depth from the LFA data the wake edge velocities must be determined. The LFA rotor wake velocity profiles contain the influences of both the rotor wake and the wake/blade interaction. We considered the wake depth to be relatively unaffected, but the edges of the actual rotor wake were difficult to identify. From the experimental data it was noted that over a rotor blade passing period the number of measurements per window was not uniform and that more measurements per window were acquired in the pressure side of the rotor wake region than in

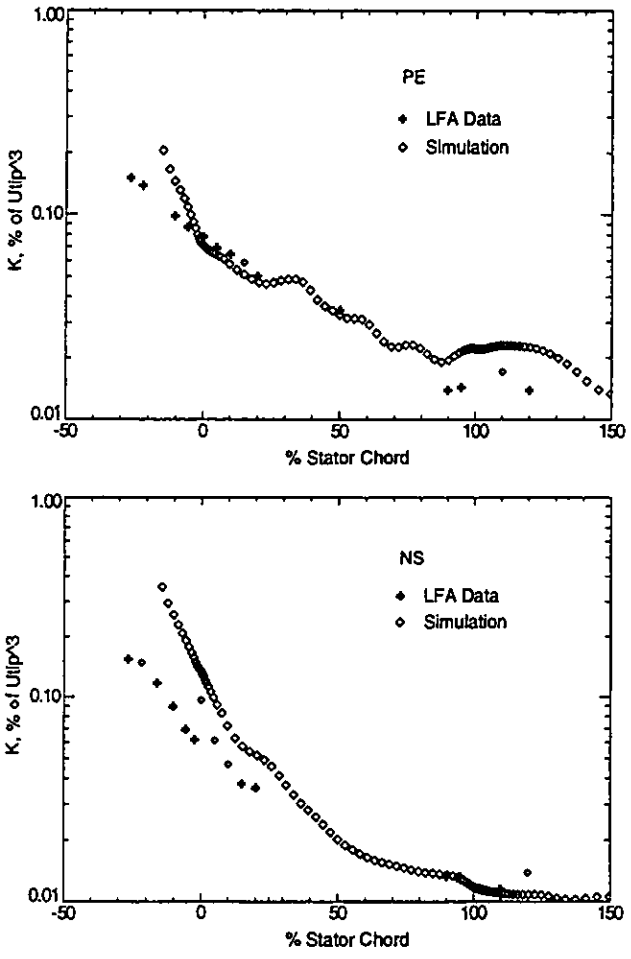

FIGURE 7. Comparison of stage LFA and simulation decay of the flux of DKE for the PE and NS operating conditions.

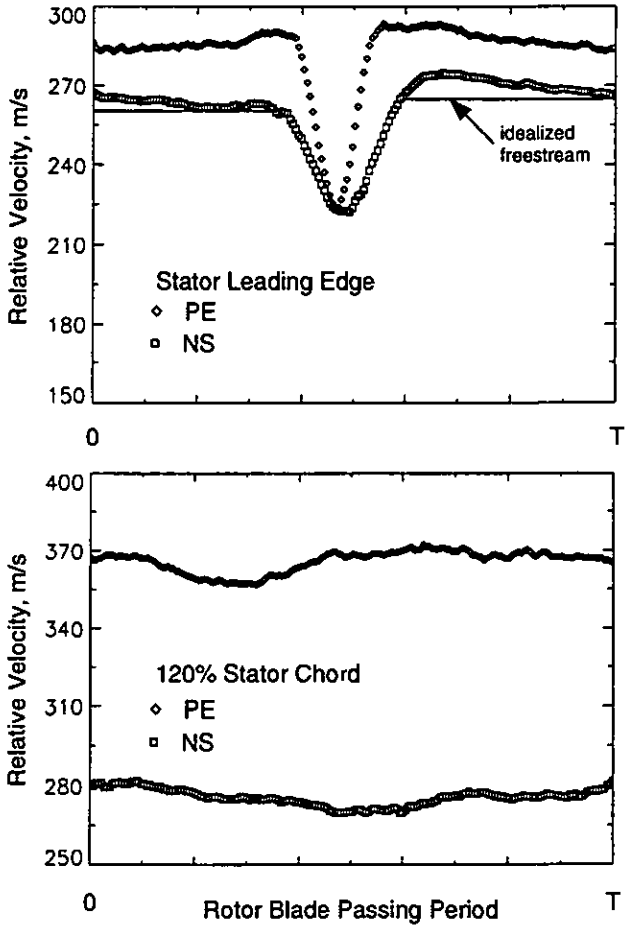

FIGURE 8. Midpitch wake profiles for PE and NS at the SLE and stator exit planes in the stage environment.

the 'core flow' region between wakes. The measurement distribution was thus used to assist in locating the edges of the rotor wake in the velocity profiles. The velocity in the regions outside of the rotor wake was considered constant and was set equal to the corresponding wake edge velocity. This results in a 'idealized' LFA rotor wake profile, see Figure 8, for which the wake/blade interaction effects are minimized. The relative wake depth for the LFA data was then calculated from the average of the wake edge velocities and the minimum wake velocity.

The relative wake depth calculated from Eqn. 8 is used to determine a wake width using Eqn. 9 and then a wake velocity profile is calculated using Eqn. 10. The wake profiles are shifted so that:

$$\int_0^T V dy|_x = \int_0^T V dy|_{SLE} \qquad \text{(EQ 11)}$$

where V is the relative velocity magnitude. Eqn. 11 ensures mass conservation as the wake profile shape changes. The relative disturbance kinetic energy is calculated from these profiles as:

$$DKE_{REL} = 0.5 V_o A_t (V - V_o)^2 \qquad \text{(EQ 12)}$$

where V_o is the time average relative velocity magnitude. Change in DKE_{REL} will be approximately proportional to the change in mixing loss. The DKE_{REL} for LFA data is calculated in a similar manner using the modified velocity profiles described previously.

A comparison between the model calculation and experimental (LFA) data at midpitch is shown in Figure 9 in terms of a) the relative wake depth and b) the relative disturbance kinetic energy. For the relative wake depth results: the curve labelled *viscous+stretching* is calculated from Eqn. 8, the curve labelled *stretching only* is calculated from Eqn. 8 with the eddy viscosity set to zero, the curve labelled *viscous only* is calculated from Eqn. 8 with the velocity ratio set to 1.0.

The predicted change in relative wake depth shows remarkably good agreement with the LFA data as shown by the curve labelled *viscous+stretching* in part a) of Figure 9. The change in relative wake depth between the stator inlet and exit planes (0 and 110% chord) is 77% for PE and 83% for NS. The *stretching only*

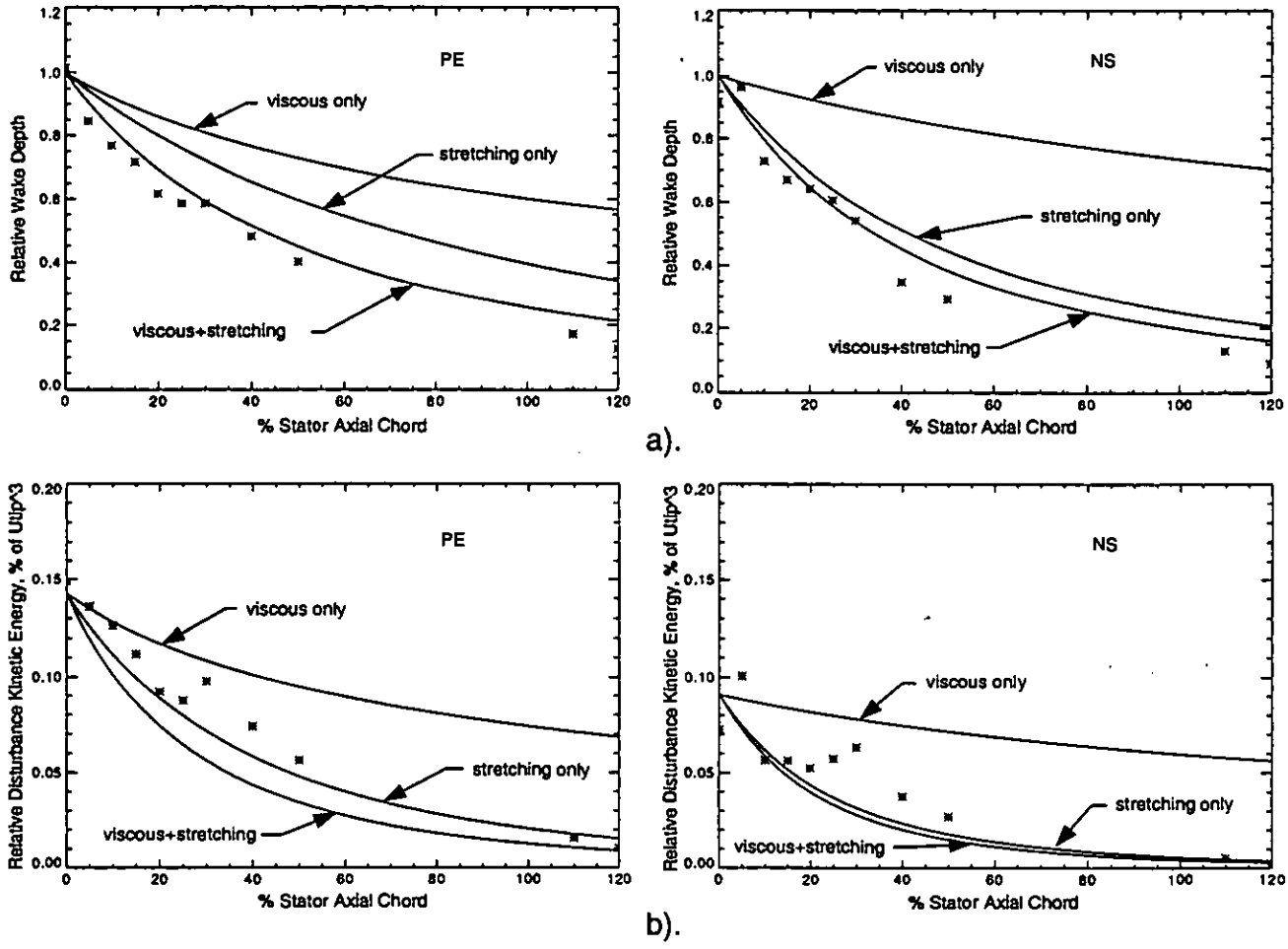

FIGURE 9. Comparison of LFA data to wake decay model predictions for the PE and NS cases.

curve shows that most of the wake depth change, 64% for PE and 78% for NS, is due to wake stretching. The model indicates that the additional relative wake depth decay is due to viscous dissipation. For comparison, the curve *viscous only* shows how an isolated rotor wake with the SLE midpitch velocity profile would decay due to viscous dissipation alone. Not only is the rotor wake decay more rapid due to the presence of the stator, but the viscous contribution to wake decay is also greatly reduced.

The DKE_{REL} results shown in part b) of Figure 9 do not agree as well with the LFA data as the relative wake depth results. This is due to both poor wake width prediction by Eqn. 9 and wake/blade interaction effects on the LFA wake profiles. However, the trends that the model predicts are correct and results from the model will be used to draw some conclusions.

The wake decay model predicts that the DKE_{REL} is reduced a total of 93% for PE and 97% for NS. The DKE_{REL} reduction due to stretching was 87% for PE and approximately 97% for NS indicating that the majority of the mixing loss has been recovered. The *viscous only* curve shows the reduction in DKE_{REL} as if the rotor was in isolation.

The differing decay rates in the rotor only and stage environment are also shown in Figure 10 which compares the decay of K in the rotor only environment to the stage environment. If exponential decay is assumed, the slope of the curves is a direct comparison of decay rate. Note the K at the rotor trailing edge is not the same for rotor only and stage environment. However, the focus is on the comparisons of the decay rate and not the absolute level of K. Inside the stator passage the stage wake decay rate is greater than the rotor only decay rate. This leads to lower DKE at the stator exit in the stage environment. This is evident by comparing the wake depth downstream of the stator for rotor-only and stage cases as shown in Figures 11 and 8 respectively.

The rotor wake decay model has been shown to be reasonably accurate by comparing to experimentally measured wake decay in the stator passage. The model can now be used to comment on the implications of the wake recovery process on stage design.

DESIGN IMPLICATIONS

The combination of Eqn. 4 for wake stretching and Eqn. 8 for wake decay, provides a simple method for predicting the benefit of wake recovery in reducing rotor wake mixing losses. The model is equally applicable to the recovery of stator wakes in a

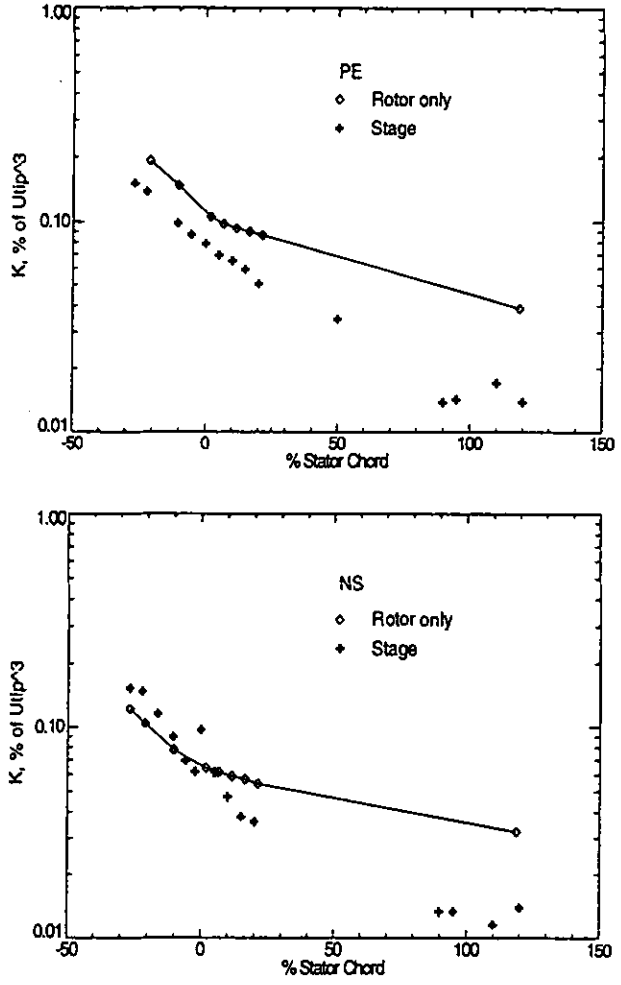

FIGURE 10. Comparison of the DKE decay in the rotor only and stage environment for the PE and NS LFA data.

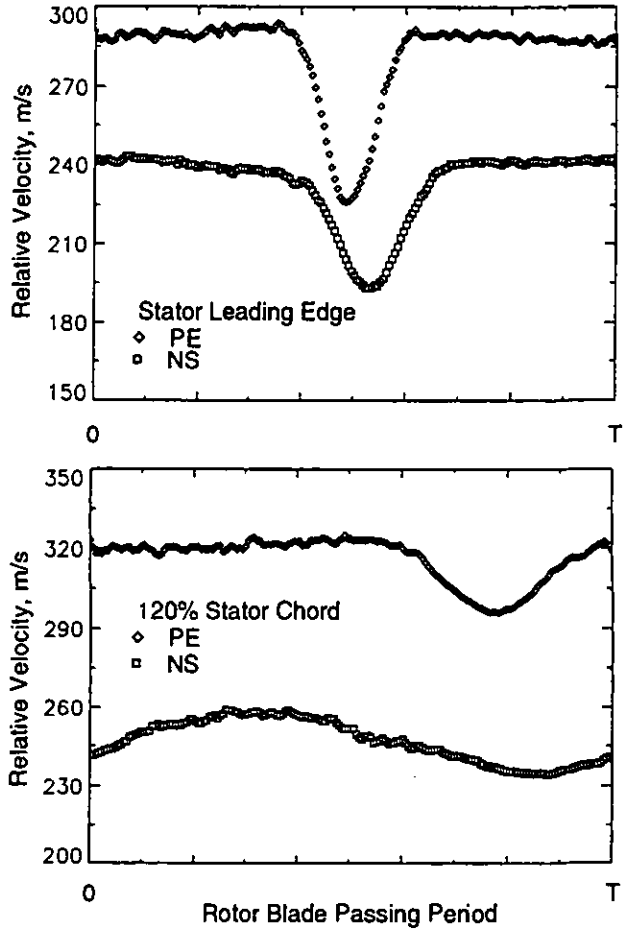

FIGURE 11. Measured wakes in the rotor only environment at the stator leading edge and 120% stator chord planes from the PE and NS LFA data.

downstream rotor.

Assuming a 2D incompressible flow, the wake decay model was used to perform a rotor wake decay audit based on the mid-pitch rotor wake profiles in the stage environment versus the entirely viscous decay of isolated rotor wakes. The results are shown in Figure 12. From the rotor TE to SLE 22% and 46% of the possible wake decay has occurred for PE and NS, respectively, all of it due to viscous mixing and thus resulting in loss. Of the remaining rotor wake decay possible at the SLE, 68% for PE and 52% for NS occurred by inviscid stretching of the rotor wake in the stator passage involving no loss. Only small amounts of rotor wake mixing loss occurred in the stator passage because of viscous mixing. This implies that using loss correlations based on isolated rotor or cascade data may be misleading for multistage design.

Since a significant amount of mixing loss occurs before the rotor wake enters the stator passage, closer axial spacing of blade rows to capture the rotor wake sooner would be beneficial. An efficiency gain due to closer axial spacing of 1.2 points was achieved in a four-stage low speed compressor (Smith, 1970). Of this efficiency gain, 0.52 points was attributed to wake recovery and the remainder attributed to other mechanisms, for example tangential variations of total pressure caused by the downstream stator imposing non-uniform back pressure on the rotor ahead of it (Smith, 1996).

Additionally, capturing the rotor wake sooner assumes that the closer spacing would not cause increased losses in the rotor and/or stator due to potential field interactions or stronger wake/blade interactions. Regarding increased rotor losses, at 75% span in this stage, the stator velocity field impact on the rotor was small. The circumferential variation of the absolute velocity at the rotor trailing edge was 2.5% as measured by the LFA system at the NS operating condition where the interaction was strongest. Because of the small interblade gap, no rotor performance measurements are possible in the stage configuration and nothing more definitive can be said about rotor performance at this time.

An effect similar to closer axial spacing could be achieved by reducing the viscous decay rate of the rotor wake. The viscous decay rate immediately downstream of the TE is dependent on the shear velocity and the static pressure differences across the wake

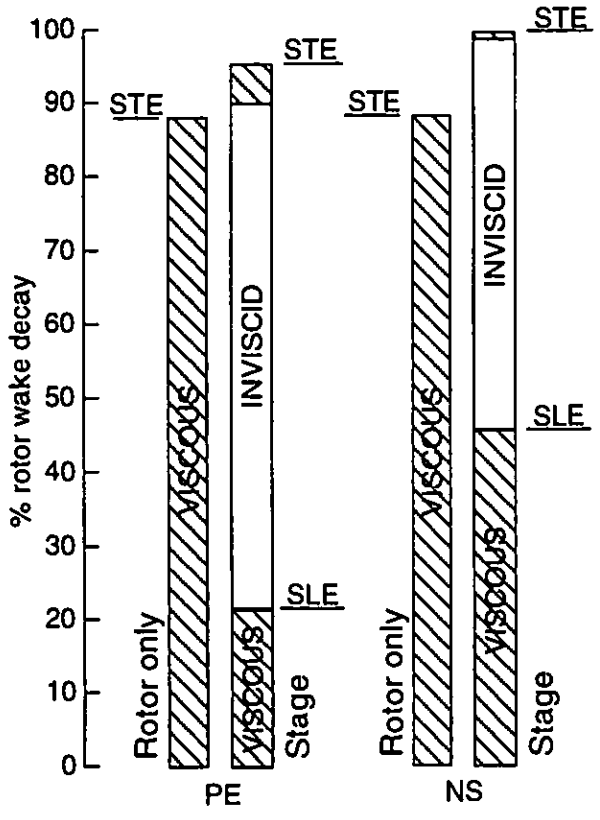

FIGURE 12. Rotor wake decay audit (0% represents the rotor trailing edge location).

(the assumption of constant static pressure across the wake does not hold in this region). A small separation at the rotor TE may reduce the shear velocity and static pressure difference and thus reduce the viscous mixing rate. This is speculative and needs further investigation.

By designing stages which use the wake recovery process to its full advantage, higher stage loading may be possible. As rotor blade loading is increased, profile loss and thus rotor wake mixing loss would also increase. However, in the stage environment a high percentage of the rotor wake mixing loss could be recovered in the stator row. This recovery would offset some of the higher rotor profile losses and thus might allow higher stage loading without incurring large efficiency penalties.

A higher percentage of mixing loss is recovered in the stator passage for the NS case relative to the PE case due to less viscous contribution to mixing in the stator and more overall wake stretching. Front loaded stators (as in the NS case) turn and stretch the wake sooner in the stator passage which further reduces the viscous decay contribution. Front loading also enhances the wake/blade response attenuation of the wake as shown at location A in Figure 5. This attenuation occurs because the stator generates a pressure response to the presence of a rotor wake passing over the surface such that the correct boundary condition is maintained on the stator surface. This wake/blade response is also a reversible process.

CONCLUSIONS

A simple model has been developed to evaluate the relative contributions of viscous dissipation and inviscid stretching to the decay of a rotor wake in a stator row. The model requires only blade geometry, inlet and exit velocity triangles, and an assumed rotor wake profile as input and is simple enough to be useful as a design tool. Results from the model compared favorably with laser anemometer data and numerical simulation results. The model correctly predicts that, within the stator row, inviscid wake stretching is the dominant rotor wake decay mechanism as opposed to viscous dissipation.

Inviscid wake decay due to stretching provides a means of tailoring a compressor stage design to avoid some of the loss associated with the entirely viscous decay of a rotor wake. This also implies that the use of isolated rotor or cascade loss correlations for multistage compressor design may be misleading. Examples of stage design features which influence the balance between viscous dissipation and wake stretching are:

- Axial spacing of blade rows

In a compressor stage, a significant amount of rotor wake decay has already occurred by viscous dissipation before the wake enters the stator row. Some of this loss can be avoided by moving the stator row closer to the rotor trailing edge.

- Reduced rotor wake shear

A reduction in the rotor wake shear will reduce the rotor wake viscous mixing in the axial gap between rotor and stator rows. Such a reduction might be achieved by designing for a small amount of separation within the rotor, thus broadening the wake width.

- Front loading of stators

Front loaded stator blades stretch the rotor wake inviscidly earlier in the stator passage and further reduce the already small amount of viscous dissipation involved in that row.

ACKNOWLEDGEMENTS

This work was done at the NASA Lewis Research Center under grant number NAG3-1302. We are grateful to Dr. Kenneth Suder for his assistance concerning the LFA system operation and Mr. Jerry Wood for many helpful suggestions for data analysis.

REFERENCES

Adamczyk, J. J., "Model Equation for Simulating Flows in Multistage Turbomachinery," ASME Paper No. 85-GT-226, 1985.

Adamczyk, J. J., "Wake Mixing in Axial Flow Compressors," ASME Paper No. 96-GT-029, 1996.

Chen, J. P., Celestina, M. L., and Adamczyk, J. J., "A New Procedure for Simulating Unsteady Flows Through Turbomachinery Blade Passages," ASME Paper No. 94-GT-151, 1994.

Deregel, P. and Tan, C. S., "Impact of Rotor Wakes on Steady-State Axial Compressor Performance," ASME Paper No. 96-GT-253, 1996.

Ding, K., "Flow Measurements Using a Laser-Two-Focus Anemometer in a High-Speed Centrifugal and a Multistage Axial Compressor," presented at the Winter Annual Meeting of ASME, Phoenix, Arizona, November, 1982.

Dunker, R. J., "Flow Measurements in the Stator Row of a Single-Stage Transonic Axial-Flow Compressor with Controlled Diffusion Stator Blades", AGARD CP-351, Viscous Effects in Turbomachines, 1983.

Hathaway, M. D., "Unsteady Flows in a Single-Stage Transonic Axial-Flow Fan Stator Row," NASA TM 88929, December 1986, (also see ASME 87-GT-226 and 87-GT-227).

Hill, P. G., Schaub, U. W., and Senoo, Y., "Turbulent Wakes in Pressure Gradients," ASME Journal of Applied Mechanics, December 1963, pp. 518-524.

Kool, P. and Hirsch, Ch., "A Prediction Scheme for the Decay of a Turbomachine Blade Wake," ASME Paper No. 82-GT-273, 1982.

Kerrebrock, J. L. and Mikolajczak, A. A., "Intra-Stator Transport of Rotor Wakes and Its Effect on Compressor Performance," ASME Journal of Engineering for Power, October 1970, pp. 359-368.

Nakayama, A., "Curvature and Pressure-Gradient Effects on a Small Defect Wake," Journal of Fluid Mechanics, Vol. 175, 1987, pp. 215-246.

Raj, R. and Lakshminarayana, B., "Characteristics of the Wake Behind a Cascade of Airfoils," Journal of Fluid Mechanics, Vol. 61, 1973, pp. 707-730.

Reid, L. and Moore, R. D., "Design and Overall Performance of Four Highly Loaded, High-Speed Inlet Stages for an Advanced High-Pressure-Ratio Core Compressor," NASA TP 1337, October 1978.

Reid, L. and Moore, R. D., "Performance of Single-Stage Axial-Flow Transonic Compressor With Rotor and Stator Aspect Ratios of 1.19 and 1.26, Respectively, and with Design Pressure Ratio of 1.82," NASA TP 1338, November 1978.

Sherman, Frederick S., **Viscous Flow**, McGraw-Hill Publishing Company, 1990.

Smith, L. H. Jr., "Wake Dispersion in Turbomachines," Journal of Basic Engineering, September 1966, pp. 688-690.

Smith, L. H. Jr., "Casing Boundary Layers in Multistage Axial-Flow Compressors," Flow Research in Blading, edited by L. S. Dzung, Elsevier Publishing Company, Amsterdam, 1970.

Smith, L. H. Jr., "Wake Ingestion Propulsion Benefit," Journal of Propulsion and Power, Vol. 9, No. 1, Jan.-Feb. 1993, pp. 74-82.

Smith, L. H. Jr., 1996 in, "Discussion of ASME Paper No. 96-GT-029: Wake Mixing in Axial Flow Compressors," 1996 ASME Turbo Expo, Birmingham, England, June 10-13.

Stauter, R. C., Dring, R. P., and Carta, F. O., "Temporally and Spatially Resolved Flow in a Two-Stage Axial Compressor: Part 1-Experiment," ASME Journal of Turbomachinery, Vol. 113, 1991, pp. 212-226.

Strazisar, A. J., Wood, J. R., Hathaway, M. D., and Suder, K. L., "Laser Anemometer Measurements in a Transonic Axial-Flow Fan Rotor," NASA TP 2879, November 1989.

Tweedt, D. L., Hathaway, M. D., and Okiishi, T. H., "Multistage Compressor Stator/Rotor Interaction," Journal of Propulsion, Vol. 1, No. 6, Nov-Dec., 1985, pp. 449-455.

Williams, M. C., "Inter and Intrablade Row Laser Velocimetry Studies of Gas Turbine Compressor Flows," ASME Journal of Turbomachinery, Vol. 110, July 1988, pp. 369-376.

APPENDIX

The kinematic model of wake stretching and the wake decay model are based on 2D incompressible flow assumptions and do not include the effects of either wake drift or radial transport. Rotor wake drift in the stator row as described by Kerrebrock and Mikolajczak (1970) is a result of the lower relative velocity of the wake fluid. Rotor wake fluid thus has a larger tangential velocity component than the free stream fluid and 'drifts' toward the stator pressure surface. A calculation of the drift velocity indicated that the maximum drift of a wake fluid particle as the wake convects through the stator passage would be less than 1/3 of the stator pitch toward the pressure surface. The entropy contours from the numerical simulations shown in Figure 13 show that the high entropy rotor wake fluid particles extend across the stator pitch, even at the stator exit. Therefore, wake decay in the stator is not primarily due to the wake fluid drifting to the pressure surface of the stator.

Radial velocities in the rotor wakes predicted by the CFD simulations were significant at the rotor trailing edge, 12% and 27% of absolute velocity for PE and NS cases respectively. However, at the stator leading edge the radial velocities were reduced to 6% and 13% of absolute velocity for PE and NS cases. The radial migration within the stator passage was 5.5% and 10.5% span for PE and NS. Therefore, the flow field was considered sufficiently two dimensional in the core spans of the compressor stator such that calculating wake decay on a geometric 75% span stream surface was considered a reasonable approximation to following a wake fluid particle.

Because the LFA system only measures two velocity components, mixing loss calculations with the LFA data must be done by assuming 2D incompressible flow. The unsteady simulations are used to estimate the error associated with these assumptions. For a rotor wake at midpitch SLE from the simulations, the 2D incompressible mixing loss calculation is in error by -38% for PE and -23% for NS as a percentage of the 3D compressible mixing loss for the rotor wake. At the STE, the error is -27% for PE and -18% for NS as a percentage of the 3D compressible mixing loss of the rotor wake at midpitch SLE. The total mixing loss is small compared to the incoming kinetic energy, so the error incurred by the assumptions is a small in absolute magnitude. The simple 2D incompressible mixing loss calculations consistently underpredict the rotor wake mixing loss.

Compressibility affects wake recovery in two ways. First, compressibility affects the mean flow velocities and it is the mean flow which determines the wake stretching. Both the LFA data and the simulation, of course, include this compressibility effect. The simple wake stretching model, which is based on an incompressible assumption, does well in predicting the wake stretching and thus indicates that compressibility is a small effect. Secondly, wake recovery is affected because of the assumption that the circulation is constant for inviscid incompressible flow. For compressible viscous flow the circulation around a material segment of mass changes as (Sherman, 1990):

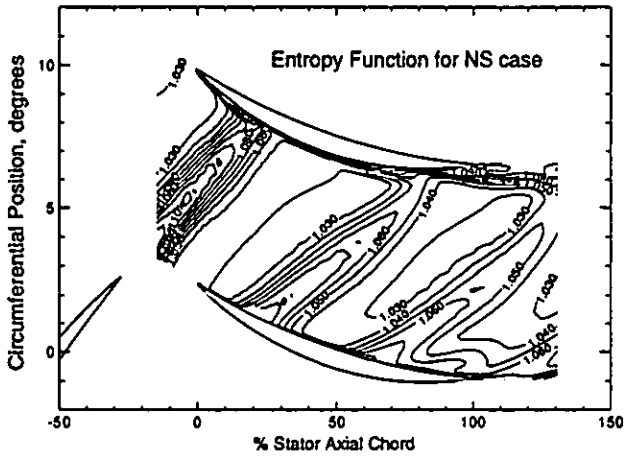

FIGURE 13. Entropy contours showing the rotor wake locations for a fixed rotor/stator position from the NS simulation.

$$\frac{d\Gamma}{dt} = \oint\left(-\frac{\nabla P}{\rho} + \frac{\nabla \bullet \tau}{\rho}\right)d\ell \qquad \text{(EQ 13)}$$

This is a line integral that encloses the segment of mass. The first term on the right hand side is zero if the density is only a function of the pressure. For a stator row where static temperature changes are small, this term should be small. The second term on the right hand side is the divergence of the stress tensor and represents the viscous impact on circulation. Because the rotor wake has decayed significantly before entering the stator row, this term is expected to be small also except possibly near the blade surfaces. Further work is needed to better quantify these effects.

In summary, wake drift and radial transport were not considered significant wake decay influences and evaluating mixing loss using 2D incompressible assumptions will show the correct trends.